Regulation of Energy Dissipation in Photosystem I by the Redox State of the Plastoquinone Pool†

David Joly and Robert Carpentier*

Groupe de Recherche en Biologie Végétale, Université du Québec à Trois-Rivières, Trois-Rivières, Québec, Canada G9A 5H7

Received December 21, 2006; Revised Manuscript Received March 12, 2007

ABSTRACT: The effect of exogenous plastoquinone (PQ) on the different deexcitation pathways of photosystem I (PSI) was investigated. Addition of oxidized decyl-plastoquinone (dPQ) and PQ-2 strongly quenched the chlorophyll (Chl) emission spectra of PSI submembrane fractions over all wavelengths. This quenching increased with the concentration of exogenous PQ added and followed the modified Stern−Volmer law. The Stern−Volmer constants found for dPQ and PQ-2 were 1.25×10^6 M^{-1} and 0.55×10^6 M^{-1}, respectively, and the fraction of fluorescence accessible to the quencher was 0.7 for both exogenous PQ. dPQ and PQ-2 also retarded the P700 photooxidation measured under limiting actinic light irradiances. Photoacoustic measurements showed that addition of dPQ increased the heat dissipation and decreased the photochemical capacity of PSI. From these results, exogenous oxidized PQ were shown to efficiently quench the Chl excited state in the PSI antenna and change the balance between Chl deexcitation pathways. Moreover, reduction of the endogenous PQ pool in whole thylakoid membranes by NADPH increased PSI fluorescence by 65%, indicating the importance of the redox state of the PQ pool on PSI energy dissipation.

In cyanobacteria and higher plants, oxygenic photosynthesis involves the light reactions of photosystems I and II (PSI[1] and PSII) working in series. While PSII is responsible for water oxidation, PSI mediates the light-driven electron transfer from plastocyanin to ferredoxin (Fd) (*1*). Reduced Fd is used by the enzyme ferredoxin:$NADP^+$ reductase (FNR) to produce NADPH required for carbon fixation (*2*). PSI is a 525 kDa protein pigment complex of the thylakoid membrane that comprises 12 core subunits and four light-harvesting proteins (Lhca1−4) forming a half-moon shape around the core (*3*). PsaA and PsaB are the central subunits of the core complex (*4*). They bind about 96 chlorophylls (Chl), 22 β-carotene, the PSI reaction center, and primary electron donor (P700) identified as a special Chl pair, two phylloquinones, and 3 [4Fe-4S] iron−sulfur clusters (*4*). Lhca1−4 are organized in dimers to form two light-harvesting complexes of PSI (LHCI): LHCI-680 composed of subunits Lhca2 and Lhca3, and LHCI-730 composed of subunits Lhca1 and Lhca4 (*5*−*7*). LHCI proteins have a unique feature among Chl-binding proteins as they contain Chl with red-shifted absorbance (*8*).

Light absorption by antenna pigments leads to the building of electronic excited states that are transferred as excitons between the pigment molecules (*9*). Trapping of an exciton by P700 induces its photooxidation and the consequent charge separation driving electron transport in PSI (*10*). In isolated reaction center (RC) preparations, the quantum yield of charge separation is close to unity (*11*). However, each exciton has also a probability to be dissipated by radiative emission or heat. Both dissipation processes compete with the photochemical reaction and decrease its quantum yield (*12, 13*). Therefore, the rate of photosynthetic electron transport depends on the respective quantum yield of each dissipative pathway.

In intact photosynthetic tissues, special mechanisms are known to reversibly increase the probability of excitons in the PSII antenna to thermally dissipate and decrease radiative dissipation (*14*). As this quenching of the Chl excited states is not linked to the photochemical trapping of excitons, these mechanisms are commonly referred to as non-photochemical quenching (NPQ) of Chl fluorescence (*15*). NPQ includes many distinct processes contributing to light adaptation and photoprotection of the photosynthetic machinery (*15*). Low lumenal pH induces protonation of LHCII, conversion of their violaxanthin pigments to zeaxanthin, and a consequent conformational change that increases thermal dissipation in PSII antennas in the so-called high-energy state quenching (qE) (*16*). Photoinhibition quenching (qI) is caused by slowly reversible damage to PSII reaction centers (*17*). Another important NPQ component is the state transition (qT), a phosphorylation-related migration of LHCII from PSII to PSI (*18*). State transition was also reported to slightly increase the antenna cross-section in PSI (*19*). Energy dissipation of PSI, however, is thought to be mainly indirectly controlled

† This work was supported by Natural Sciences and Engineering Research Council of Canada (NSERC).

* Author for correspondence. E-mail: Robert.Carpentier@uqtr.ca. Phone: 1-819-376-5011 ext 3300. Fax: +1-819-376-5057.

[1] Abbreviations: ΔA_{830}, absorbance changes at 830 nm; CeT, cyclic electron transport; Chl, chlorophyll; DBMIB, dibromothymoquinone; dPQ, decyl-plastoquinone; f_a, fraction of fluorescence accessible to the quencher; FNR, ferredoxin:NADPH reductase; K_{SV}, Stern−Volmer constant; LHC, light harvesting complex; NPQ, non-photochemical quenching; P700, primary electron donor of photosystem I; PA, photoacoustic; PQ, plastoquinone; PQ_{ex}, exogenous plastoquinone; PS, photosystem; qE, energy-dependent quenching; qI, photoinhibitory quenching; qT, state transition quenching; RC, reaction center.

10.1021/bi602627d CCC: $37.00
Published on Web 04/14/2007

by NPQ mechanisms acting on PSII (*20*). Information on quenching of Chl excited states in PSI is restricted to the view that $P700^+$ is an excellent non-photochemical quencher (*21*). Recently, $NADP^+$-dependent reversible conformation changes of PSI were also proposed to affect energy dissipation (*22*).

Oxidized plastoquinone (PQ) molecules are known as non-photochemical quenchers of Chl excited states of PSII (*23*−*25*). Their reduction at the PSII acceptor side was proposed to be reflected by the increase in fluorescence from I to P steps within 1 s during fluorescence induction (FI) kinetics, as reduced plastoquinones (PQH_2) cannot quench Chl excited states (*26*, *27*). PQ-type fluorescence quenching would correspond to about 20−25% of the maximal fluorescence yield in thylakoids (*25*, *26*). Because LHCI shows important similarity with PSII antennas in their structure and pigment binding properties (*3*, *28*), PQ should also affect fluorescence and energy dissipation in PSI. Artificial exogenous quinones in their oxidized form were shown to act as quenchers of Chl excited states of PSI, and consequently quenched fluorescence and decreased the rate of P700 photooxidation under limiting illumination (*27*, *29*). However, the capacity of the endogenous PQ pool to alter energy dissipation in PSI has not been examined.

In the present work, we studied the effect of exogenous PQ on PSI submembrane fractions. Our work revealed that exogenously added PQ molecules were highly efficient in fluorescence quenching, increased thermal dissipation of Chl excited states, retarded the photooxidation of PSI, and decreased the photochemical capacity of PSI RC. Reduction of the endogenous PQ pool in thylakoid membranes caused a major increase in Chl fluorescence of PSI. An important impact of the PQ pool redox state in PSI dissipative pathways is thus shown. The results are discussed in terms of a possible role of PQ in the regulation of PSI activity.

MATERIALS AND METHODS

Isolation of Photosynthetic Materials and Sample Preparation. Thylakoids and PSI submembrane fractions were isolated from fresh spinach leaves obtained from a local market, according to the procedure of Peters et al. (*30*) with some modifications (*31*). These stroma lamella preparations retain the cytochrome b_6f complex, a full complement of plastocyanin, and a Chl/P700 ratio of 260 (*30*), and they were devoid of PSII polypeptides (*22*). Chl concentration was determined in 80% acetone according to Porra et al. (*32*). The isolated fractions with approximately 1−2 mg of Chl/mL were suspended in a medium containing 20 mM Tricine-KOH buffer (pH 7.8), 10 mM NaCl, 10 mM KCl, and 5 mM $MgCl_2$ and stored at −80 °C until use. Unless mentioned, the same buffer was used as a measurement medium.

For experiments done under anaerobiosis, photosynthetic samples were incubated 45 min in the dark in the presence of 10 mM glucose, 50 units/mL glucose oxidase, and 1000 units/mL catalase. dPQ was obtained from Sigma-Aldrich (D7786) and dissolved in ethanol. PQ-2 and PQ-9 were provided by Dr. Jerzy Kruk (Department of Plant Physiology and Biochemistry, Jagiellonian University, Poland) in ethanol solution at a concentration of 1 mM. Chemical structures of these PQ molecules are presented in Figure 1. For all measurements, ethanol concentration was kept below 1% (v/v).

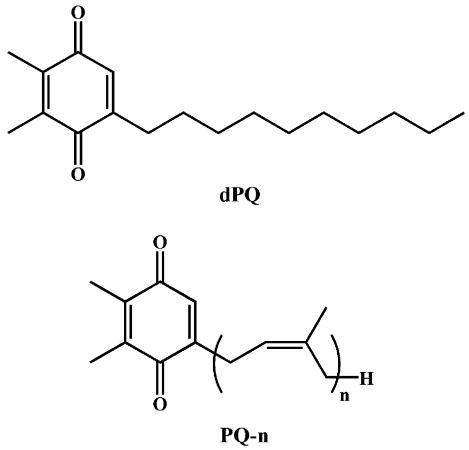

FIGURE 1: Chemical structures of dPQ and PQ-*n*. Endogenous type of PQ corresponds to PQ-9.

Fluorescence Measurements. The room temperature (298 K) and low temperature (77 K) spectra of fluorescence emission were measured with a Perkin-Elmer LS55 spectrofluorimeter equipped with a red-sensitive photomultiplier R928. Chl fluorescence was excited at 436 nm. The excitation and emission spectral widths were fixed at 5 and 2.5 nm, respectively. Emission spectra were corrected according to the photomultiplier sensitivity using the correction factor spectrum provided by Perkin-Elmer. The Chl content of the samples was adjusted to 5 μg/mL. Low temperature spectra were measured as reported previously (*33*) in the presence of 60% glycerol.

Absorbance Changes at 830 nm (ΔA_{830}). Absorbance changes at 830 nm were assayed using a PAM Chl fluorometer (Walz, Effeltrich, Germany) equipped with ED-P700DW dual-wavelength emitter-detector unit. White actinic light for measurements with the PAM device was obtained from a Fiber-Lite source (Microview, Thornhill, ON, Canada) and controlled by an electronic shutter. The signals of absorbance changes were recorded using the Walz Data Acquisition System DA100. Chl concentration was 66 μg/mL during the measurements of absorbance changes of PSI submembrane fractions, which were done with an optical path of 1.065 mm. The measurements were performed in the presence of 3 mM methyl viologen to prevent charge recombination between $P700^+$ and reduced acceptor side intermediates of PSI. Experimental conditions were the same for the experiments using thylakoid membranes, except that Chl concentration was 100 μg/mL and 100 μM diuron was added to prevent reduction of P700 by electrons coming from PSII during measurements.

Photoacoustic Spectroscopy. For the measurements of photoacoustic (PA) signal, 150 μL of PSI fractions diluted to 250 μg of Chl/mL in the final resuspension buffer was absorbed on a nitrocellulose filter (Millipore Corp., AA type, 0.8 μm pore size) in the presence of 5 mM ascorbate and 0.3 mM 2,6-dichlorophenolindophenol (DCIP). The filter was cut to the proper dimensions for introduction in the PA cell (MTEC Photoacoustic, Ames, IA). PA measurements were made with a laboratory-built PA spectrometer (*34*). The light beam from a 150 W xenon lamp (ILC Technology, Sunnyvale, CA) passing through a monochromator (Photon Tech-

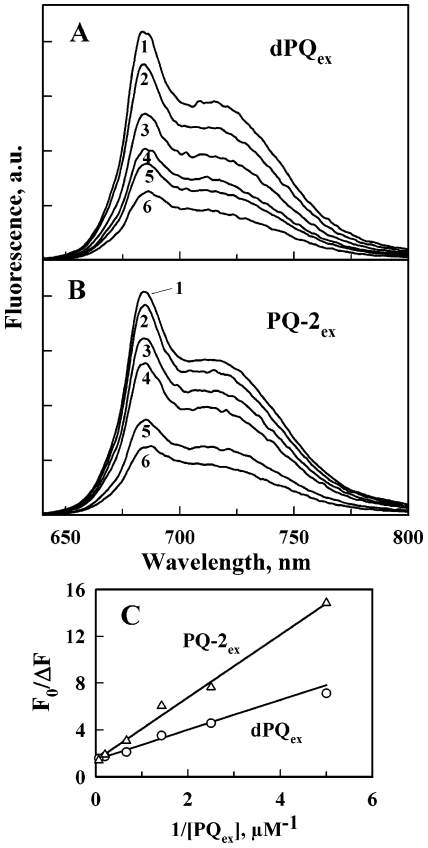

FIGURE 2: Fluorescence emission spectra measured in isolated PSI submembrane fractions at room temperature with the addition of dPQ (A) or PQ-2 (B) at a concentration of 0 (1), 0.2 (2), 0.7 (3), 1.5 (4), 5 (5), and 15 μM (6). (C) Modified Stern−Volmer plots of Chl fluorescence quenching by dPQ (circles) or PQ-2 (triangles). Chl fluorescence was integrated from 640 to 800 nm using the emission spectra. For other details, see Materials and Methods.

nology International Inc., Brunswick, NJ, model PTI 101-001SF) to obtain light at 680 nm was modulated with a mechanical chopper at a frequency of 35 Hz. The light intensity was controlled with neutral density filters. Saturating background illumination (150 W/m^2) from a KL1500 projector (Walz, Effeltrich, Germany) was used to completely oxidize P700, thus converting all PSI reaction centers into a photochemically inactive state.

RESULTS

Figure 2 shows the fluorescence emission spectra of photosystem I submembrane fractions in the absence of additive or in the presence of various concentrations of exogenous plastoquinone molecules (PQ_{ex}). The spectra of untreated PSI submembrane fractions showed a maximum at 684 nm and a shoulder around 725 nm, as described before (*27*, *35*). Addition of a low concentration (0.2 μM) of dPQ or PQ-2 quenched 14% and 7% of the fluorescence spectra, respectively. The importance of the fluorescence quenching increased with amount of PQ_{ex} added, and at 15 μM up to 70% of the emission was lost. Also, the extent of the quenching was similar for all wavelengths of the emission spectra. However, addition of various concentrations of PQ-9, the type of PQ found in vivo in thylakoids, could only slightly quench the emission spectra of PSI (not shown). It should be noted that added quinones did not alter the absorption properties of the PSI submembrane fractions.

Variation of fluorescence quenching can be described by the Stern−Volmer law (*36*):

$$\frac{F_0}{F} = 1 + K_{SV}[Q] \quad (1)$$

where F_0 and F are the Chl fluorescence emission integrated from 640 to 800 nm in the absence or in the presence of PQ_{ex}, respectively, K_{SV} is the Stern−Volmer quenching constant, and [Q] is the concentration of the fluorescence quencher, which is PQ_{ex} in the present case and will be therefore replaced by [PQ_{ex}]. However, the relationship between F_0/F and [PQ_{ex}] is not linear when a fraction of the fluorescence is not accessible to the quencher (*23*). This condition was observed in our experiments (not shown). However, the Stern−Volmer equation can be modified to take into account the fluorescence accessible ($F_{0,a}$) and inaccessible ($F_{0,i}$) to the quencher. The fluorescence in the absence of quencher becomes

$$F_0 = F_{0,a} + F_{0,i} \quad (2)$$

Thus, the fraction of fluorescence accessible to the quencher (f_a) is defined as

$$f_a = \frac{F_{0,a}}{F_0} \quad (3)$$

The above gives rise to a modified Stern−Volmer equation (*23*, *37*, *38*):

$$\frac{F_0}{\Delta F} = \frac{1}{f_a K_{SV}[PQ_{ex}]} + \frac{1}{f_a} \quad (4)$$

where ΔF is the fluorescence intensity difference in the absence and presence of PQ_{ex}. By plotting $F_0/\Delta F$ against [PQ_{ex}]$^{-1}$, f_a is found from the intercept, which is f_a^{-1}, and K_{SV} is obtained from the slope of the graph (f_a^{-1} K_{SV}^{-1}). K_{SV} characterizes the efficiency of the quencher.

Figure 2C shows that the modified Stern−Volmer equation provided linear traces for dPQ and PQ-2. In both cases, f_a values were 0.7 and a K_{SV} of 1.25 × 10^6 M^{-1} and 0.55 × 10^6 M^{-1} was calculated for dPQ and PQ-2, respectively.

The quenching of Chl excited states by PQ_{ex} should limit the yield of exciton transfer between Chl molecules in the antenna and affect the rate of P700 photooxidation, particularly under nonsaturating illumination. Figure 3 shows the traces of ΔA_{830} induced by low irradiance (4.6 W/m^2) in PSI submembrane fractions. Positive changes in ΔA_{830} indicate photooxidation of P700. Increasing concentrations of added dPQ from 15 μM to 300 μM decreased the rate of P700 photooxidation, which delayed the establishment of a stable and complete level of P700 photooxidation. However, the total magnitude of ΔA_{830} was not significantly altered by the addition of dPQ. P700 photooxidation kinetics were fitted with a first-order kinetics to verify its dependency on the concentration of added dPQ. The rate constant of P700 photooxidation decreased with the concentration of added dPQ from 0 to 300 μM, and an almost optimal effect was observed at 50 μM oxidized quinone. (Figure 3, inset). It should be noted that the Chl concentration was more than 10 times higher compared to the fluorescence experiments. This explains why a higher concentration of exogenous

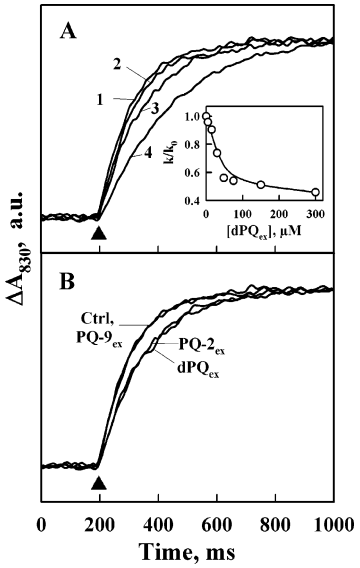

FIGURE 3: Original traces of light-induced increase in absorbance at 830 nm measured in isolated PSI submembrane fractions (A) with the addition of 0 (1), 15 (2), 30 (3), and 300 μM (4) of dPQ or (B) with the addition of 30 μM of different types of PQ molecules. The upward arrow indicates actinic light turned on. Inset: Dependency of the photooxidation rate constant (k) on the concentration of added dPQ. Traces of light-induced increase in ΔA_{830} were fitted with first-order kinetics, and calculated values of k were normalized with the rate found for the control ($k_0 = 0.009$ ms^{-1}).

dPQ was needed to obtain a significant effect on the P700 photooxidation. 30 μM of PQ-2 and dPQ retarded similarly the P700 photooxidation, while PQ-9 did not induce significant changes in the P700 photooxidation kinetics (Figure 3B).

As PQ_{ex} were shown to decrease the yield of radiative dissipation of Chl excited states in the antenna and to slow the delivery of excitons to the PSI reaction center, an alternative dissipative pathway must be favored, which should be thermal dissipation. To confirm this hypothesis, photoacoustic spectroscopy was used to monitor thermal dissipation. Heat release was studied at various measuring light intensities in either the absence or the presence of 150 μM dPQ. The modulated measuring beam was used to obtain a steady state of thermal dissipation (Q_c) under a different level of nonsaturating PSI excitation (Figure 4, inset). Under these conditions, the modulated beam caused the closing of part of the reaction centers, the fraction of closed centers increasing with measuring beam intensity. Therefore, only part of the absorbed energy was stored in photochemical reactions and thus not released. Then, strong nonmodulated white light was applied to completely oxidize P700, thus converting all PSI RC into a photochemically inactive state. Consequently, the fraction of absorbed modulated light energy converted into thermal emission reached its maximal level (Q_m). Turning off the saturating white light brought back the PA signal to its steady state Q_c (Figure 4, inset). Using the values of Q_c and Q_m, the photosynthetic energy storage yield (ϕ_I) at a given modulated light intensity can be calculated (*39*−*41*):

$$\phi_I = \frac{(Q_m - Q_c)}{Q_m} \times 100\% \qquad (5)$$

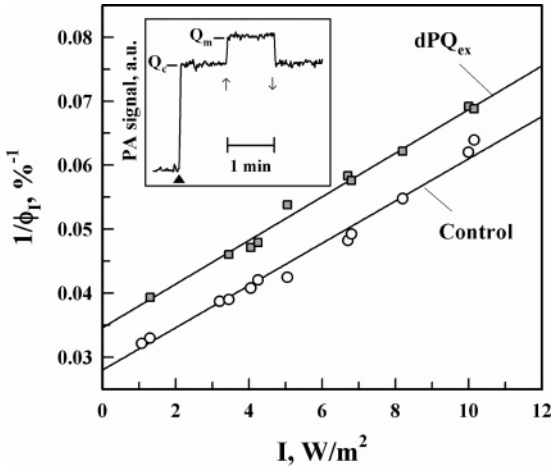

FIGURE 4: Dependency of the reciprocal of the energy storage yield on the modulated light intensity for PSI submembrane fractions in the absence (open circles) or in the presence (closed squares) of 150 μM dPQ_{ex}. Inset: Photoacoustic signal from PSI submembrane fractions aspired on a nitrocellulose filter. Upward triangle indicates modulated light on. Upward and downward arrows indicate strong white light on and off, respectively.

As the fraction of closed reaction centers increased with the intensity of modulated light, the fraction of absorbed energy used for photochemical reactions as measured by ϕ_I also decreased. As a result, for both untreated and treated (150 μM dPQ) PSI, ϕ_I decreased by about 40−45% as light intensity was raised from 1.1 to 10.2 W/m^2 (results not shown). However, ϕ_I was smaller for dPQ treated PSI than in control at all light intensities.

To characterize further the effect of PQ_{ex} on the PA signal, the relationship between the energy storage yield and the measuring beam intensity (I) was studied. Plotting the reciprocal of ϕ_I versus I leads to a linear relationship where the intercept represents the maximal photosynthetic energy storage yield (ϕ_m) extrapolated to a modulated light intensity of zero, thus when all reactions centers are in the open state (*42*). Further extrapolation of the relation to the abscissa provides the modulated light intensity that closes half of the photosystems (i_{50}). This relationship corresponds to the following equation:

$$\frac{1}{\phi_I} = \frac{1}{\phi_m}\left(\frac{I}{i_{50}} + 1\right) \qquad (6)$$

where the slope is $(\phi_m i_{50})^{-1}$ (*42*).

Figure 4 shows the ϕ_I^{-1} vs I plot for PSI in the absence or presence of 150 μM dPQ. Both untreated and treated PSI had the same slope, but addition of dPQ increases the value of the intercept. This corresponds to a decrease of the maximal photosynthetic energy storage yield from 36% to 29% for control and dPQ-treated PSI, respectively, while the i_{50} increased from 8.5 W/m^2 to 10 W/m^2. The above indicates an inhibition of energy storage by about 20% at the dPQ concentration used. This seems a weak inhibition compare to the strong fluorescence quenching reported in Figure 2. However, this can be expected as the final effective concentration of added dPQ during PA measurements is difficult to estimate. Indeed, a fraction of solubilized dPQ is lost by aspiration of the liquid medium during the filtration of the PSI preparations on the nitrocellulose filter (*42*) and

the final concentration of PSI in terms of Chl concentration becomes very high thus leading to a low dPQ/Chl ratio.

Even though the above data demonstrate that exogenous PQ molecules added to isolated PSI submembrane fractions influence energy dissipation of PSI, it would be interesting to verify the impact of the endogenous PQ pool on PSI in a more intact and complete system such as whole thylakoid membranes. The endogenous PQ pool of thylakoid membranes can be specifically reduced under anaerobiosis by the addition of NADPH (*43*, *44*). Reduction of the PQ pool by NADPH was shown to produce a strong increase in the amplitude of the O-J rise of Chl FI observed within the first milliseconds of illumination (data not shown) (*43*, *44*).

At room temperature, fluorescence measurements in thylakoids are mainly influenced by PSII (*45*, *46*). Such measurements are efficient to probe the PQ redox state but cannot give clear information about the influence of PQ on PSI. Nonetheless, the unique spectral properties of red Chl present only in PSI can be used to distinguish between PSII and PSI contributions to the emission spectra of thylakoids at cryogenic temperature. At room temperature, PSII fluorescence from vibrational sublevels overlaps with red Chl fluorescence of PSI at 720−750 nm, and PSI contributions can hardly be separated from PSII (*47*). At cryogenic temperature, the vibrational bands of PSII fluorescence are lost and PSI fluorescence comes from its red Chl, because uphill energy transfer from red Chl to bulk antenna Chl is not efficient at this temperature. Hence, two clearly separated emission bands emerge at 680 and 735 nm, coming from PSII and PSI, respectively (*48*−*51*). Therefore, NADPH can be used to reduce the endogenous PQ pool in whole thylakoid membranes and the subsequent 77 K fluorescence emission spectra will show the effect of oxidized vs reduced PQ pool on the quenching of Chl excited state for both PSII and PSI.

Figure 5A shows that reduction of the endogenous PQ pool by NADPH increased both PSII and PSI emission bands by about 40% and 65%, respectively. Conversely, 1 μM of added dPQ quenched about 45% of both PSII and PSI fluorescence. The action of added dPQ was reversed if thylakoids were incubated in the presence of both NADPH and dPQ, which yields to an increased emission spectrum similar to thylakoids incubated in the presence of NADPH alone.

Moreover, the ability of oxidized dPQ_{ex} to retard P700 photooxidation in isolated thylakoids under low irradiance (4.6 W/m^2) is demonstrated in Figure 5B. As observed in PSI submembrane fractions, increasing concentrations of added dPQ decreased the rate of P700 photooxidation. The decrease in its first-order rate constant was similar to what was observed with PSI submembrane fractions (Figure 5B, inset).

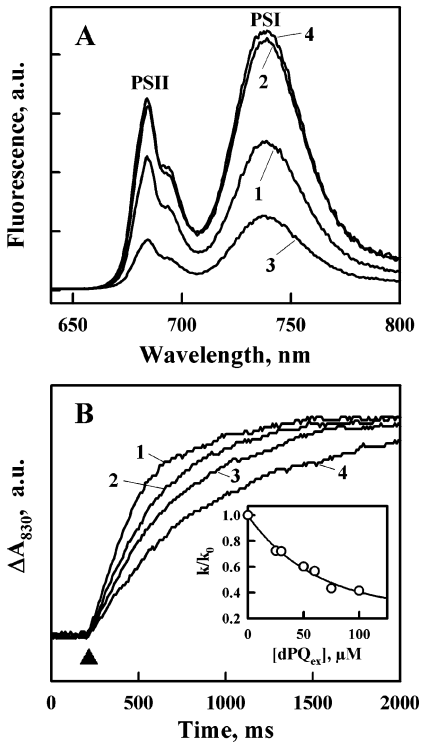

FIGURE 5: Influence of dPQ_{ex} on energy dissipation of PSI in thylakoid membranes. (A) Fluorescence emission spectra measured in isolated thylakoids at 77 K without additive (1) or in the presence of 500 μM NADPH (2), 1 μM dPQ (3), or both 500 μM NADPH and 1 μM dPQ (4). Incubation of the sample before measurement was carried out under anaerobiosis as described in Materials and Methods. (B) Original traces of light-induced increase in absorbance at 830 nm measured at room temperature in isolated thylakoids with the addition of 0 (1), 30 (2), 60 (3), and 100 μM (4) of dPQ. The upward arrow indicates actinic light turned on. Inset: Dependency of the photooxidation rate constant (k) on the concentration of added dPQ. Traces of light-induced increase in ΔA_{830} were fitted with first-order kinetics, and calculated values of k were normalized with the rate found for the control ($k_0 = 0.0034$ ms^{-1}).

DISCUSSION

A number of special mechanisms are known to control energy utilization in photosynthesis by modulating heat dissipation of PSII (*14*). These mechanisms provide the flexibility needed by the photosynthetic apparatus to adapt itself to a wide variety of environmental light conditions and to limit photoinhibitory damage (*15*, *20*). However, little is known about PSI contribution to regulative and photoprotective mechanisms, and this subject is rarely discussed in the literature (*22*, *52*). This is mainly because PSI activity is thought to be only indirectly controlled by the regulation of PSII activity (*20*). Nonetheless, addition of artificial quinones such as dibromothymoquinone (DBMIB), 2,5-dichloro-*p*-benzoquinone (DCBQ), and duroquinone (DQ) were recently shown to quench the excited states of Chl in PSI submembrane fractions (*27*). To our knowledge, the present study is the first to show that exogenous and endogenous plastoquinone molecules may control the utilization of absorbed light energy in PSI.

Among the different types of plastoquinone used, PQ-9 did not exhibit any significant effect on PSI fluorescence or P700 photooxidation (Figure 3). The same absence of effect of PQ-9 was also previously observed by Bojko and co-workers (*53*, *54*) when they assessed the reduction of different quinones by FNR. The above is explained by the formation of micelles by PQ-9 molecules in the polar measurement buffer owing to their long aliphatic chain (Figure 1), which prevented them to interact efficiently with the photosynthetic membrane.

Addition of dPQ and PQ-2 caused an important decrease in the fluorescence emission spectra of PSI submembrane fractions. This fluorescence quenching was well described by the modified Stern−Volmer equation (Figure 2), which takes into account that a part of the fluorescence is not

accessible to the quencher (*23*). The Stern−Volmer constants found, quantifying the quencher efficiency, were twice to four times higher than those found by Rajagopal et al. (*27*) for the most efficient artificial quinone tested, DBMIB. The PSI submembrane fractions used in the present study are composed of about 260 Chl/RC and 11 endogenous PQ/RC (*30*). The impact of the addition of 11 dPQ/RC, corresponding to about 0.25 μM dPQ, can be estimated from Figure 2C and results into a nearly 20% quenching of the PSI fluorescence, which points toward a possible physiological significance of the endogenous PQ pool effects on PSI energy dissipation.

As shown by Rajagopal et al. (*27*), the quenching of Chl excited states of PSI observed in fluorescence spectra leads also to a delay in the P700 photooxidation measured under limiting light. The same effect was observed in this study in the presence of exogenous dPQ or PQ-2 (Figure 3). This indicates that oxidized PQ_{ex} molecules in the neighborhood of PSI retard the migration of excitons between antenna Chls toward the RC by increasing the probability of nonradiative dissipation of their excited state. The above was confirmed by the measurement of heat dissipation using photoacoustic spectroscopy.

Photoacoustic measurements under different light intensities permit the simultaneous assessment of heat dissipation and photosynthetic capacity of PSI. Exogenous dPQ produced a decrease in the energy storage yield (ϕ_I) and an increase in the half-saturation light intensity of energy storage (i_{50}). These changes are due to an increase of thermal dissipation under nonsaturating illumination in the presence of exogenous dPQ owing to the capacity of oxidized dPQ to statically quench the Chl excited states in PSI antennas. In Figure 4, the photoacoustic data lead to parallel slopes of ϕ_I vs I relationships for untreated and dPQ_{ex}-treated PSI. The above shows that the addition of oxidized dPQ to PSI submembrane fractions mimics a decrease in the measuring light intensity because it increased the fraction of absorbed light energy dissipated as heat before it can reach a reaction center. Then, for the same measuring light intensity, the energy storage yield was decreased after the addition of oxidized dPQ.

The most striking observation of this work is the demonstration of the increased PSI fluorescence in whole thylakoid membranes at 77 K, where the contribution of PSII and PSI can be clearly distinguished, upon reduction of the endogenous PQ pool by NADPH (Figure 5). This effect cannot be attributed to state transition as no ATP needed for LHCII phosphorylation was added to the thylakoids and the maximal level of fluorescence (F_m) measured by fluorescence induction rise was not significantly affected by the incubation of thylakoids in the presence of NADPH (data not shown) (*55*, *56*). Additionally, the retardation of P700 photooxidation by dPQ_{ex} measured in PSI submembrane fractions was also observed in isolated thylakoids (Figure 5B). Clearly, the redox state of the endogenous PQ pool can have a significant effect on PSI energy dissipation. An illustration of the action of oxidized PQ on Chl excited states of PSI antennas is presented in Figure 6.

It is likely that endogenous PQ molecules are contact with the antenna of PSI complexes in the thylakoid membranes. Even if rapid diffusion of PQ is thought to be limited to small microdomains close to PSII, slow long-range diffusion is also expected (*57*). Joliot et al. (*58*) observed a slow redistribution of PQ molecules between granal and stromal pools with a half-time of 6 s. Thus, the redox state of PQ in the vicinity of PSI can influence PSI reactions in vivo.

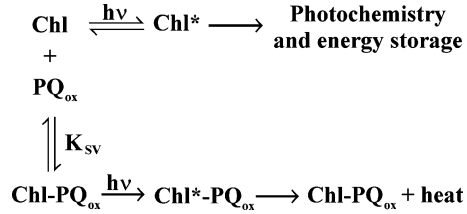

FIGURE 6: Incompetitive inhibition of the PSI energy storage yield by oxidized PQ (PQ_{ox}) molecules. Chl*, excited Chl; hν, photon.

The observed effects of the PQ pool could contribute to light adaptation and photoprotection. Under some stress conditions, like freezing stress or heat stress, the Benson−Calvin cycle is partially inhibited (*59*, *60*), resulting in an accumulation of NADPH. This would indeed result in the accumulation of reduced PQ molecules through the action of NADPH dehydrogenase, Fd-quinone oxidoreductase pathway, or FNR diaphorase activity. Oppositely to oxidized PQ molecules, these reduced PQs would contribute to increase the photosynthetic capacity of PSI required to activate the cyclic electron transport (CET). The latter is known to rapidly increase the proton gradient across the thylakoid membranes, resulting in the activation of photoprotective energy-dependent NPQ mechanisms (*61*, *62*). Moreover, reduced PQs are known as efficient scavengers of superoxide ions generated in thylakoid membranes during light stress (*63*) and would then additionally contribute to a direct photoprotective effect.

The influence of the redox state of the endogenous PQ pool on the fluorescence of PSI could also introduce some artefacts in the measurements of variable Chl fluorescence, which was attributed exclusively to PSII. In intact leaves, PSI can contribute up to 40% of F_0 and 14% of F_m for emission wavelength higher than 700 nm (*45*). If the redox state of the PQ pool is affected by a treatment prior to the measurement or during a measurement over a sufficient time scale, some changes in the fluorescence pattern could be wrongly attributed to PSII. However, the variable part of the fluorescence induction rise within the first second of excitation should not be affected by the effects of PQ on PSI since the redistribution of the PQ molecules in the thylakoid membranes operates with a half-time of 6 s (*58*).

In conclusion, the present study shows that the redox state of the endogenous PQ pool has a significant influence in the balance of PSI dissipative pathways. This mechanism is likely to improve the maximal PSI activity under conditions where PSII activity is high and could contribute to an enhancement of the PSI turnover rate when CET routes are favored.

ACKNOWLEDGMENT

The authors thank Dr. Jerzy Kruk for providing PQ molecules and Johanne Harnois for helpful professional assistance. D.J. was recipient of graduate fellowships from Fonds Québécois de Recherche sur la Nature et les Technologies and NSERC.

REFERENCES

1. Chitnis, P. R. (2001) Photosystem I: Function and Physiology, *Annu. Rev. Plant Physiol. Plant Mol. Biol. 52*, 593−626.
2. Herrmann, R. G. (1999) Biogenesis and Evolution of Photosynthetic (Thylakoid) Membranes, *Biosci. Rep. 19*, 355−365.
3. Ben-Shem, A., Frolow, F., and Nelson, N. (2003) Crystal structure of plant photosystem I, *Nature 426*, 630−635.
4. Jordan, P., Fromme, P., Witt, H. T., Klukas, O., Saenger, W., and Krausz, N. (2001) Three-dimensional structure of cyanobacterial photosystem I at 2.5Å resolution, *Nature 411*, 909−917.
5. Ganeteg, U., Strand, A., Gustafsson, P., and Jansson, S. (2001) The Properties of the Chlorophyll a/b-Binding Proteins Lhca2 and Lhca3 Studied in Vivo Using Antisense Inhibition, *Plant Physiol. 127*, 150−158.
6. Jansson, S., Andersen, B., and Scheller, H. V. (1996) Nearest-Neighbor Analysis of Higher-Plant Photosystem I Holocomplex, *Plant Physiol. 112*, 409−420.
7. Kargul, J., Nield, J., and Barber, J. (2003) Three-dimensional Reconstruction of a Light-harvesting Complex I- Photosystem I (LHCI-PSI) Supercomplex from the Green Alga Chlamydomonas reinhardtii. Insights into light harvesting for PSI, *J. Biol. Chem. 278*, 16135−16141.
8. Melkozernov, A. N. (2001) Excitation energy transfer in Photosystem I from oxygenic organisms, *Photosynth. Res. 70*, 129−153.
9. Gobets, B., and van Grondelle, R. (2001) Energy transfer and trapping in photosystem I, *Biochim. Biophys. Acta 1507*, 80−99.
10. van Grondelle, R., Dekker, J. P., Gillbro, T., and Sundstrom, V. (1994) Energy transfer and trapping in photosynthesis, *Biochim. Biophys. Acta 1187*, 1−65.
11. Sun, A. S. K., and Sauer, K. (1971) Pigment systems and electron transport in chloroplasts I. Quantum requirements for the two light reactions in spinach chloroplasts, *Biochim. Biophys. Acta 234*, 399−414.
12. Buschmann, C., and Kocsányi, L. (1989) Light-induced heat production correlated with fluorescence and its quenching mechanisms, *Photosynth. Res. 21*, 129−136.
13. Butler, W. L. (1978) Energy Distribution in the Photochemical Apparatus of Photosynthesis, *Annu. Rev. Plant Physiol. 29*, 345−378.
14. Horton, P., Ruban, A. V., and Walters, R. G. (1996) Regulation of light harvesting in green plants, *Annu. Rev. Plant Physiol. Plant Mol. Biol. 47*, 655−684.
15. Muller, P., Li, X. P., and Niyogi, K. K. (2001) Non-Photochemical Quenching. A Response to Excess Light Energy, *Plant Physiol. 125*, 1558−1566.
16. Demmig-Adams, B., and Adams, III, W. W. (1996) The role of xanthophyll cycle carotenoids in the protection of photosynthesis, *Trends Plant Sci. 1*, 21−26.
17. Osmond, B., Badger, M., Maxwell, K., Bjorkman, O., and Leegood, R. (1997) Too many photons: photorespiration, photoinhibition and photooxidation, *Trends Plant Sci. 2*, 119−121.
18. Allen, J. F. (1992) Protein-Phosphorylation in Regulation of Photosynthesis, *Biochim. Biophys. Acta 1098*, 275−335.
19. Haldrup, A., Jensen, P. E., Lunde, C., and Scheller, H. V. (2001) Balance of power: a view of the mechanism of photosynthetic state transitions, *Trends Plant Sci. 6*, 301−305.
20. Ort, D. R. (2001) When There Is Too Much Light, *Plant Physiol. 125*, 29−32.
21. Bukhov, N. G., and Carpentier, R. (2003) Measurement of photochemical quenching of absorbed quanta in photosystem I of intact leaves using simultaneous measurements of absorbance changes at 830 nm and thermal dissipation, *Planta 216*, 630−638.
22. Rajagopal, S., Bukhov, N. G., Tajmir-Riahi, H. A., and Carpentier, R. (2003) Control of energy dissipation and photochemical activity in photosystem I by NADP-dependent reversible conformational changes, *Biochemistry 42*, 11839−11845.
23. Karukstis, K. K., Boegeman, S. C., Fruetel, J. A., Gruber, S. M., and Terris, M. H. (1987) Multivariate analysis of Photosystem II fluorescence quenching by substituted benzoquinones and naphthoquinones, *Biochim. Biophys. Acta 891*, 256−264.
24. Vasil'ev, S., Wiebe, S., and Bruce, D. (1998) Non-photochemical quenching of chlorophyll fluorescence in photosynthesis. 5-hydroxy-1,4-naphthoquinone in spinach thylakoids as a model for antenna based quenching mechanisms, *Biochim. Biophys. Acta 1363*, 147−156.
25. Vernotte, C., Etienne, A. L., and Briantais, J.-M. (1979) Quenching of the system II chlorophyll fluorescence by the plastoquinone pool, *Biochim. Biophys. Acta 545*, 519−527.
26. Boisvert, S., Joly, D., and Carpentier, R. (2006) Quantitative analysis of the experimental O-J-I-P chlorophyll fluorescence induction kinetics. Apparent activation energy and origin of each kinetic step, *FEBS J. 273*, 4770−4777.
27. Rajagopal, S., Egorova, E. A., Bukhov, N. G., and Carpentier, R. (2003) Quenching of excited states of chlorophyll molecules in submembrane fractions of Photosystem I by exogenous quinones, *Biochim. Biophys. Acta 1606*, 147−152.
28. Jansson, S. (1999) A guide to the Lhc genes and their relatives in Arabidopsis, *Trends Plant Sci. 4*, 236−240.
29. Lee, J. W., Zipfel, W., and Owens, T. G. (1992) Quenching of chlorophyll excited states in photosystem I by quinones: Stern-Volmer analysis of fluorescence and photochemical yield, *J. Lumin. 51*, 79−89.
30. Peters, F. A. L. J., Van Spanning, R., and Kraayenhof, R. (1983) Studies on well coupled Photosystem I-enriched subchloroplast vesicles. Optimization of ferredoxin-mediated cyclic photophosphorylation and electric potential generation, *Biochim. Biophys. Acta 724*, 159−165.
31. Boucher, N., Harnois, J., and Carpentier, R. (1990) Heat-stress stimulation of flow in a photosystem I submembrane fraction, *Biochem. Cell. Biol. 68*, 999−1004.
32. Porra, R. J., Thompson, W. A., and Kriedemann, P. E. (1989) Determination of accurate extinction coefficients and simultaneous-equations for assaying chlorophyll-a and chlorophyll-b extracted with 4 different solvents - Verification of the concentration of chlorophyll standards by atomic-absorption spectroscopy, *Biochim. Biophys. Acta 975*, 384−394.
33. Rajagopal, S., Bukhov, N. G., and Carpentier, R. (2002) Changes in the structure of chlorophyll-protein complexes and excitation energy transfer during photoinhibitory treatment of isolated photosystem I submembrane particles, *J. Photochem. Photobiol. B: Biol. 67*, 194−200.
34. Velitehkova, M. Y., and Carpentier, R. (1994) Variable thermal dissipation in a Photosystem I submembrane fraction, *Photosynth. Res. 40*, 263−268.
35. Rajagopal, S., Joly, D., Gauthier, A., Beauregard, M., and Carpentier, R. (2005) Protective effect of active oxygen scavengers on protein degradation and photochemical function in photosystem I submembrane fractions during light stress, *FEBS J. 272*, 892−902.
36. Valeur, B. (2002) *Molecular fluorescence: principles and applications*, Wiley-VCH, Weinheim.
37. Lakowicz, J. R. (1983) *Principles of fluorescence spectroscopy*, Plenum Press, New York.
38. Lehrer, S. S. (1971) Solute perturbation of protein fluorescence. The quenching of the tryptophyl fluorescence of model compounds and of lysozyme by iodide ion, *Biochemistry 10*, 3254−3263.
39. Carpentier, R., Larue, B., and Leblanc, R. M. (1984) Photoacoustic spectroscopy of *Anacystis nidulans* III. Detection of photosynthetic activities, *Arch. Biochem. Biophys. 228*, 534−543.
40. Malkin, S., and Cahen, D. (1979) Photoacoustic spectroscopy and radiant energy conversion: Theory of the effect with special emphasis on photosynthesis, *Photochem. Photobiol. 29*, 803−813.
41. Malkin, S. (2000) The photoacoustic effect in leaves and its applications, in *Probing photosynthesis: Mechanisms, regulation and adaptation* (Yunus, M., Pathre, U., and Mohanty, P., Eds.) pp 484−524, Taylor & Francis, London.
42. Carpentier, R., Leblanc, R. M., and Mimeault, M. (1989) Photoacoustic detection of photosynthetic energy storage in Photosystem II submembrane fractions, *Biochim. Biophys. Acta 975*, 370−376.
43. Haldimann, P., and Tsimilli-Michael, M. (2002) Mercury inhibits the non-photochemical reduction of plastoquinone by exogenous NADPH and NADH: evidence from measurements of the polyphasic chlorophyll a fluorescence rise in spinach chloroplasts, *Photosynth. Res. 74*, 37−50.
44. Haldimann, P., and Tsimilli-Michael, M. (2005) Non-photochemical quenching of chlorophyll a fluorescence by oxidised plastoquinone: new evidences based on modulation of the redox state of the endogenous plastoquinone pool in broken spinach chloroplasts, *Biochim. Biophys. Acta 1706*, 239−249.

45. Franck, F., Juneau, P., and Popovic, R. (2002) Resolution of the Photosystem I and Photosystem II contributions to chlorophyll fluorescence of intact leaves at room temperature, *Biochim. Biophys. Acta 1556*, 239−246.
46. Lazár, D. (2006) The polyphasic chlorophyll *a* fluorescence rise measured under high intensity of exciting light, *Funct. Plant Biol. 33*, 9−30.
47. Franck, F., Dewez, D., and Popovic, R. (2005) Changes in the room-temperature emission spectrum of chlorophyll during fast and slow phases of the Kautsky effect in intact leaves, *Photochem. Photobiol. 81*, 431−436.
48. Bredenkamp, G. J., and Baker, N. R. (1990) Modification of excitation energy distribution to photosystem I by protein phosphorylation and cation depletion during thylakoid biogenesis in wheat, *Photosynth. Res. 23*, 111−117.
49. Siffel, P., Hunalova, I., and Rohacek, K. (2000) Light-induced quenching of chlorophyll fluorescence at 77 K in leaves, chloroplasts and Photosystem II particles, *Photosynth. Res. 65*, 219−229.
50. Percival, M. P., and Baker, N. R. (1985) Comparison of chlorophyll fluorescence emission characteristics of wheat leaf tissue and isolated thylakoids as a function of excitation wavelength, *Plant, Cell Environ. 8*, 41−48.
51. Samson, G., and Bruce, D. (1995) Complementary changes in absorption cross-sections of Photosystems I and II due to phosphorylation and Mg2+-depletion in spinach thylakoids, *Biochim. Biophys. Acta 1232*, 21−26.
52. Bukhov, N. G., Rajagopal, S., and Carpentier, R. (2002) Characterization of P700 as a photochemical quencher in isolated Photosystem I particles using simultaneous measurements of absorbance changes at 830 nm and photoacoustic signal, *Photosynth. Res. 74*, 295−302.
53. Bojko, M., and Wieckowski, S. (1999) NADPH and ferredoxin: $NADP^+$ oxidoreductase-dependent reduction of quinones and their reoxidation, *Phytochemistry 50*, 203−208.
54. Bojko, M., Kruk, J., and Wieckowski, S. (2003) Plastoquinones are effectively reduced by ferredoxin:$NADP^+$ oxidoreductase in the presence of sodium cholate micelles Significance for cyclic electron transport and chlororespiration, *Phytochemistry 64*, 1055−1060.
55. Bellafiore, S., Barneche, F., Peltier, G., and Rochaix, J. D. (2005) State transitions and light adaptation require chloroplast thylakoid protein kinase STN7, *Nature 433*, 892−895.
56. Zer, H., Vink, M., Shochat, S., Herrmann, R. G., Andersson, B., and Ohad, I. (2003) Light Affects the Accessibility of the Thylakoid Light Harvesting Complex II (LHCII) Phosphorylation Site to the Membrane Protein Kinase(s), *Biochemistry 42*, 728−738.
57. Kirchhoff, H., Horstmann, S., and Weis, E. (2000) Control of the photosynthetic electron transport by PQ diffusion microdomains in thylakoids of higher plants, *Biochim. Biophys. Acta 1459*, 148−168.
58. Joliot, P., Lavergne, J., and Beal, D. (1992) Plastoquinone compartmentation in chloroplasts 1. Evidence for domains with different rates of photo-reduction, *Biochim. Biophys. Acta 1101*, 1−12.
59. Susanne, R., Christoph, G., and Krause, G. H. (1987) Inactivation of the photosynthetic carbon reduction cycle in isolated mesophyll protoplasts subjected to freezing stress, *Photosynth. Res. 14*, 137−145.
60. David, Law, R., and Crafts-Brandner, S. J. (1999) Inhibition and Acclimation of Photosynthesis to Heat Stress Is Closely Correlated with Activation of Ribulose-1,5-Bisphosphate Carboxylase/Oxygenase, *J. Plant. Physiol. 120*, 173−182.
61. Miyake, C., Shinzaki, Y., Miyata, M., and Tomizawa, K. I. (2004) Enhancement of Cyclic Electron Flow Around PSI at High Light and its Contribution to the Induction of Non-Photochemical Quenching of Chl Fluorescence in Intact Leaves of Tobacco Plants, *Plant Cell Physiol. 45*, 1426−1433.
62. Miyake, C., Horiguchi, S., Makino, A., Shinzaki, Y., Yamamoto, H., and Tomizawa, K. I. (2005) Effects of Light Intensity on Cyclic Electron Flow Around PSI and its Relationship to Non-photochemical Quenching of Chl Fluorescence in Tobacco Leaves, *Plant Cell Physiol. 46*, 1819−1830.
63. Kruk, J., Jemiola-Rzeminska, M., Burda, K., Schmid, G. H., and Strzalka, K. (2003) Scavenging of superoxide generated in photosystem I by plastoquinol and other prenyllipids in thylakoid membranes, *Biochemistry 42*, 8501−8505.

BI602627D